Antcin-A Modulates Epithelial-to-Mesenchymal Transition and Inhibits Migratory and Invasive Potentials of Human Breast Cancer Cells via p53-Mediated miR-200c Activation

DOI 10.1055/a-0942-2087
Planta Med 2019; 85: 755–765

Publishing House and Copyright:
© 2019 by
Georg Thieme Verlag KG
Rüdigerstraße 14
70469 Stuttgart
ISSN 0032-0943

Thieme

Thieme

Antcin-A Modulates Epithelial-to-Mesenchymal Transition and Inhibits Migratory and Invasive Potentials of Human Breast Cancer Cells via p53-Mediated miR-200c Activation

Authors
K. J. Senthil Kumar[1], M. Gokila Vani[1], Han-Wen Hsieh[2], Chin-Chung Lin[2], Sheng-Yang Wang[1,3]

Affiliations
1 Department of Forestry, National Chung Hsing University, Taichung, Taiwan
2 Taiwan Leader Biotech Company, Taipei, Taiwan
3 Agricultural Biotechnology Research Center, Academia Sinica, Taipei, Taiwan

Key words
antcin-A, *Antrodia cinnamomea*, Fomitopsidaceae, breast cancer, epithelial-to-mesenchymal transition, miR-200c, ZEB1, p53

received February 25, 2019
revised May 21, 2019
accepted May 23, 2019

Bibliography
DOI https://doi.org/10.1055/a-0942-2087
Published online June 11, 2019 | Planta Med 2019; 85: 755–765 © Georg Thieme Verlag KG Stuttgart · New York | ISSN 0032-0943

Correspondence
Prof. Sheng-Yang Wang
Department of Forestry, National Chung Hsing University
250, Kou Kuang Rd, Taichung 40227, Taiwan
Phone: + 88 64 22 85 03 33, Fax: + 88 64 22 86 29 60
taiwanfir@dragon.nchu.edu.tw

ABSTRACT

Antcin-A (ATA) is a steroid-like phytochemical isolated from the fruiting bodies of a precious edible mushroom *Antrodia cinnamomea*. We previously showed that ATA has strong anti-inflammatory and anti-tumor effects; however, other possible bioactivities of this unique compound remain unexplored. In the present study, we aimed to investigate the modulation of epithelial-to-mesenchymal transition (EMT), anti-migration, and anti-invasive potential of ATA against human breast cancer cells *in vitro*. Human breast cancer cell lines, MCF-7 and MDA-MB-231, were incubated with ATA for 24 h. Wound healing, trans-well invasion, western blot, q-PCR, F-actin staining, and immunofluorescence assays were performed. We found that treatment with ATA significantly blocked EMT processes, as evidenced by upregulation of epithelial markers (E-cadherin and occludin) and downregulation of mesenchymal markers (N-cadherin and vimentin) via suppression of their transcriptional repressor ZEB1. Next, we found that ATA could induce miR-200c, which is a known player of ZEB1 repression. Further investigations revealed that ATA-mediated induction of miR-200c is associated with transcriptional activation of p53, as confirmed by the fact that ATA failed to induce miR-200c or suppress ZEB1 activity in p53 inhibited cells. Further *in vitro* wound healing and trans-well invasion assays support that ATA could inhibit migratory and invasive potentials of breast cancer cells, and the effect was likely associated with induced phenotypic modulation. Taken together, the present study suggests that antcin-A could be a lead phyto-agent for the development of anti-metastatic drug for breast cancer treatment.

Introduction

Metastatic breast cancer is one of the most common malignancies diagnosed in women worldwide and ranks as the second most-common cancer-related death, surpassing lung cancer. In 2018, 2 million women were diagnosed with breast cancer and 622 000 died of breast cancer. It was predicted that by 2030, more than 2.6 million women will be diagnosed and 817 000 will die from this disease globally [1]. According to the American Cancer Society, the 5-y relative survival rate of metastasized breast cancer remains very poor (20–27 %) [2] and the incidence and mortality rates are climbing every year in some parts of the world, especially the low- and middle-income countries [3]. Several sequential steps are involved in metastasis of tumor cells, including EMT, reduction of cell-cell adhesion, alteration in the extracellular matrix, invasion, evasion, and MET [4]. Among them, EMT is recognized as the first step and is associated with disruption of intracellular tight junctions and loss of cell-cell adhesion, resulting in loss of epithelial features and gain of mesenchymal morphology. In particular, loss of epithelial adherent junction proteins such as E-cadherin, occludin, ZO-1, cytokeratin, and entatin with a con-

ABBREVIATIONS

ATA	antcin-A
ELISA	enzyme-linked immunosorbent assay
EMT	epithelial-to-mesenchymal transition
F-actin	filamentous actin
FITC	fluorescein isothiocyanate
GAPDH	glyceraldehyde 3-phosphate dehydrogenase
HBCCs	human breast cancer cells
MCF-7^{TGF}	MCF-7 cells stimulated with TGF-β1
MEM	minimum essential medium
MET	mesenchymal-to-epithelial transition
miRNA	micro RNA
PVDF	polyvinylidene difluoride
q-PCR	quantitative PCR
RIPA	radioimmunoprecipitation assay
RPMI	Roswell Park Memorial Institute
TAM	tamoxifen
TGF-β1	transforming growth factor beta 1
ZEB1	zinc finger E-box binding homeobox 1
ZO-1	zonula occludens-1

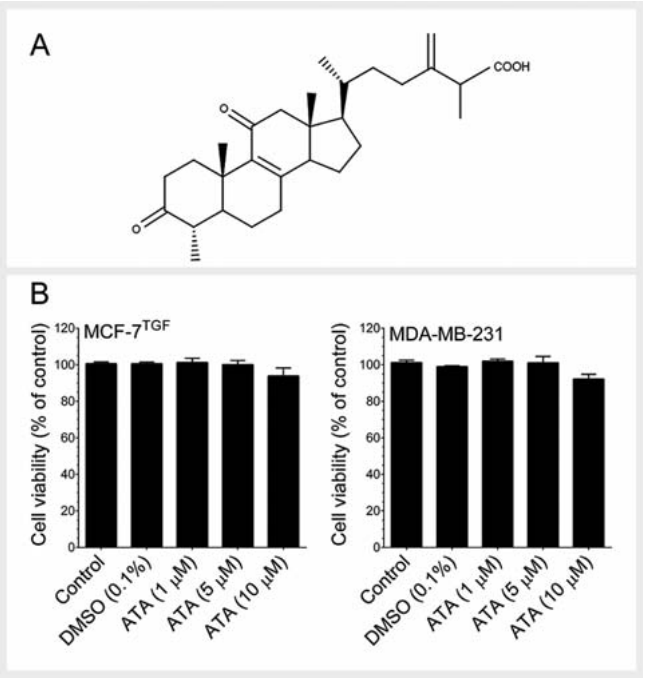

▶ **Fig. 1** Chemical structure and cytotoxic effects of ATA. **A** Chemical structure of ATA. IUPAC name: (6R)-2-methyl-3-methylidene-6-[(4S,5S,10S,13R,14R,17R)-4,10,13-trimethyl-3,11-dioxo-2,4,5,6,7,12,14,15,16,17-decahydro-1H-cyclopenta[a]phenanthren-17-yl] heptanoic acid; molecular formula: $C_{29}H_{42}O_4$; molecular weight: 454.651. **B** MCF-7 and MDA-MB-231 cells were incubated with increasing concentrations of ATA (1–10 µM) for 24 h. Cell viability was determined by MTT colorimetric assay. The percentage of cell viability was calculated by the absorption of control cells (0.1% DMSO) as 100%. The data are reported as mean ± SD of 3 independent experiments.

comitant gain in mesenchymal markers, including N-cadherin, vimentin, fibronectin, α-SMA, and β-catenin is evident [5].

miRNAs are small, noncoding RNAs that play a functional role in the regulation of gene expression at the post-transcriptional level. They have been implicated in tumorigenesis and cancer progression, including cancer cell proliferation, metastasis, cancer stem cell differentiation, and other biological functions [6]. Although, the role of miRNAs in tumorigenesis is well established, only recently have reports elucidated miRNAs as promoters or suppressors of metastasis [7]. Recent studies have revealed that members of the miRNA-200 family such as miR-200a, miR-200b, miR-200c, miR-141, and miR-429 have been shown to regulate EMT through directly targeting transcriptional repressors of E-cadherin, ZEB-1, and ZEB-2 in various cancers [8], including breast cancer [9]. A large number of phytochemicals have been studied and are potent miRNA regulatory agents against breast cancer, whereas several phytochemicals have yet to be tested against metastatic breast cancers [10].

Antrodia cinnamomea (Fomitopsidaceae) is a widely used medicinal mushroom in Taiwan that has long been used as a health-promoting remedy by the indigenous people [11]. In traditional Chinese medicine, *A. cinnamomea* is used as a folk remedy to treat various human illnesses, including liver disease, drug and food intoxication, diarrhea, abdominal pain, hypertension, and itchy skin [12]. Mounting scientific evidence confirming its various pharmacological activities, including anti-cancer, immunomodulatory, anti-inflammation, anti-oxidant, anti-mutagenic, anti-microbial, anti-diabetic, anti-aging, hepatoprotective, and neuroprotective effects [12–15]. The multiple pharmacological activities of *A. cinnamomea* are thought to be the result of a reservoir of several bioactive compounds that include terpenoids, polysaccharides, benzenoids, benzoquinone derivatives, succinic and maleic derivatives, lignans, nucleic acids, and steroids [13, 15].

We previously reported that ATA (▶ **Fig. 1A**), a steroid-like phytochemical isolated from the fruiting bodies of *A. cinnamomea*, inhibits inflammation in lung cells via mimicking as a glucocorticoid receptor agonist [16]; however, other bioactivities of this unique compounds were poorly examined. In the present study, we investigated the anti-metastatic potential of ATA against a TGF-β1-induced estrogen receptor-positive human breast epithelial cancer cell line (MCF-7) and a triple-negative HBCC line (MDA-MB-231), and the molecular mechanisms were revealed.

Results

Prior to anti-metastatic investigation, the cytotoxic effect of ATA on HBCCs was determined. MTT colorimetric assay exhibit that the cell viability was unaffected by ATA up to a concentration of 10 µM for 24 h treatment in both MCF-7 ($p = 0.067$) and MDA-MB-231 ($p = 0.052$) cells (▶ **Fig. 1B**). Next, we investigated the EMT regulatory effects of ATA in MCF-7 and MDA-MB-231 cells. We previously reported that exposure of MCF-7 cells to TGF-β1 reduced cell-cell interactions and modified them to exhibit a mesenchymal-like phenotype, a characteristic feature of EMT [17]. Hence, the TGF-β-induced MCF-7 cells were referred as MCF-7^{TGF}. To determine whether ATA could modulate cell scattering,

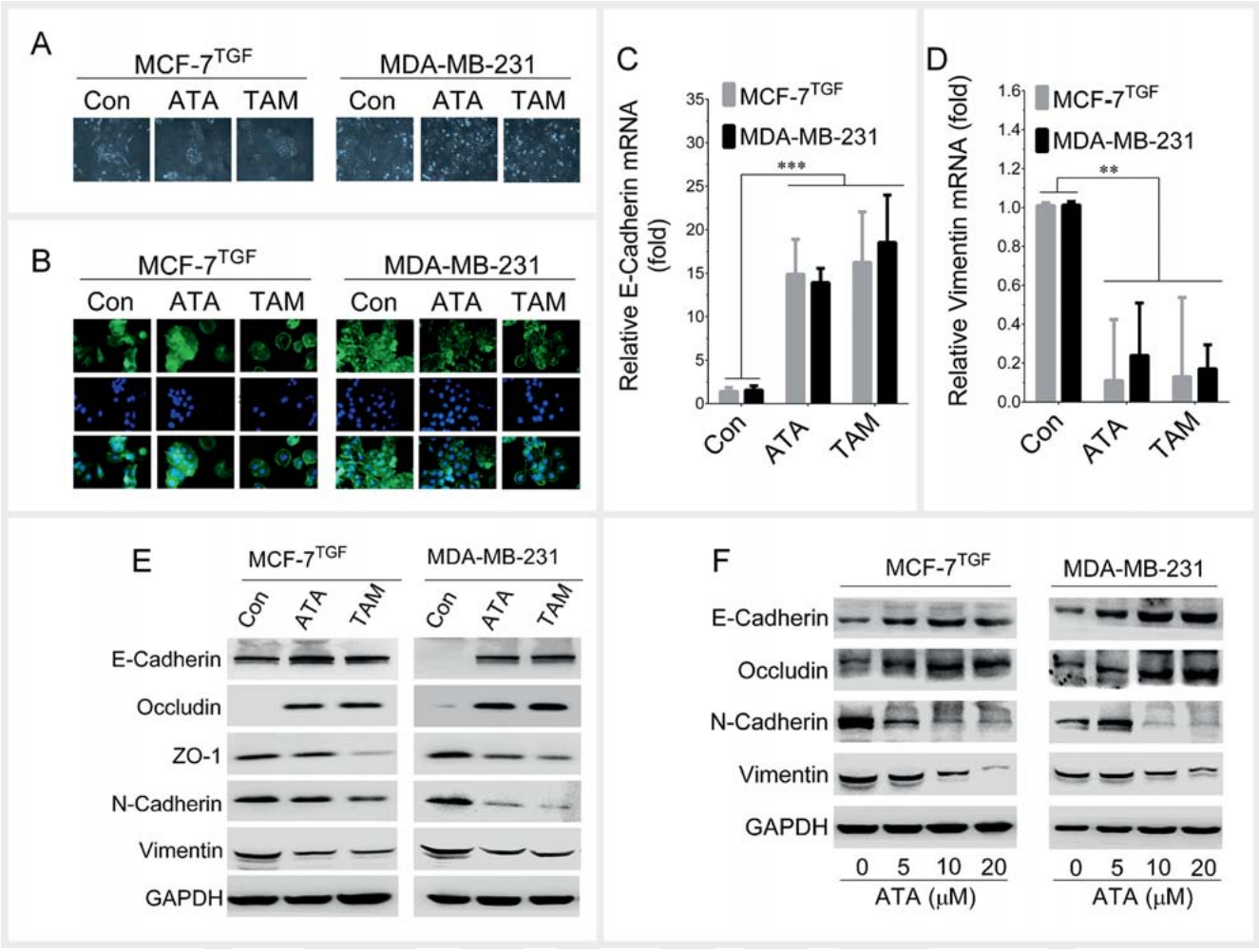

▶ **Fig. 2** ATA blocked EMT in HBCCs. MCF-7 cells were pre-treated with ATA (10 μM) or TAM (5 μM) for 2 h prior to stimulation with TGF-β1 (20 ng/mL) for 28 h. In parallel, MDA-MB-231 cells were incubated with ATA (10 μM) or TAM (5 μM) for 24 h. **A** Morphological changes were examined by phase-contrast microscope. **B** Cytoskeleton remodeling was determined by F-actin expression in FITC-conjugated phalloidin stained cells. **C** and **D** mRNA expression levels of epithelial and mesenchymal marker genes, E-cadherin, and vimentin were quantified by q-PCR analysis. **E** Protein expression levels of epithelial and mesenchymal markers including E-cadherin, occludin, ZO-1, N-cadherin, and vimentin were determined by western blot analysis. GAPDH was used as an internal loading control. **F** Cells were incubated with increasing concentrations of ATA (5, 10, and 20 μM). Total protein extracts were prepared. The effect of ATA on protein expression levels of epithelial and mesenchymal markers was determined in a dose-dependent manner. MCF-7^{TGF} represents MCF-7 cells were induced by TGF-β1 (10 ng/mL). Values represent the mean ± SD of 3 independent experiments. Statistical significance $^{***}p < 0.001$ and $^{**}p < 0.01$ compared to control vs. sample treatment groups.

MCF-7 cells were treated with either ATA (10 μM) or the known anti-metastatic drug TAM (5 μM) [18] for 24 h. The TGF-β1-stimulated cells displayed a fibroblast-like mesenchymal appearance, whereas co-treatment with ATA or TAM significantly blocked the TGF-β1-induced phenotypic changes in MCF-7 cells (▶ **Fig. 2A**). Next, we examined whether ATA had an effect on the highly metastatic cell line MDA-MB-231. Interestingly, we found that treatment with ATA or TAM modulated the phenotypic changes in MDA-MB-231 cells from a mesenchymal-like morphology to an epithelial-like morphology (▶ **Fig. 2A**). To further clarify the phenotypic modulations by ATA, cytoskeleton remodeling was examined by F-actin using fluorescence-based phallotoxin assay. As shown in ▶ **Fig. 2B**, MCF-7^{TGF} and control MDA-MB-231 cells expressed strong and polarized F-action, whereas reduced F-actin was observed in ATA-treated cells (▶ **Fig. 2B**). These data strongly support the notion that ATA modulates phenotypic transition in HBCCs.

To further clarify whether the ATA-mediated phenotypic changes in MCF-7^{TGF} or MDA-MB-231 cells resulted from dysregulation of EMT regulatory genes, we examined the mRNA expression levels of epithelial marker E-cadherin and mesenchymal marker vimentin in MCF-7^{TGF} and MDA-MB-231 cells. q-PCR analysis showed that treatment with ATA significantly increased E-cadherin expression in MCF-7^{TGF} and MDA-MB-231 cells (▶ **Fig. 2C**), whereas the mesenchymal marker vimentin was significantly inhibited by ATA in both cell lines (▶ **Fig. 2D**). A similar effect was also observed in cells treated with TAM in a same course of time. Next, we examined the effect of ATA on EMT regulatory genes at

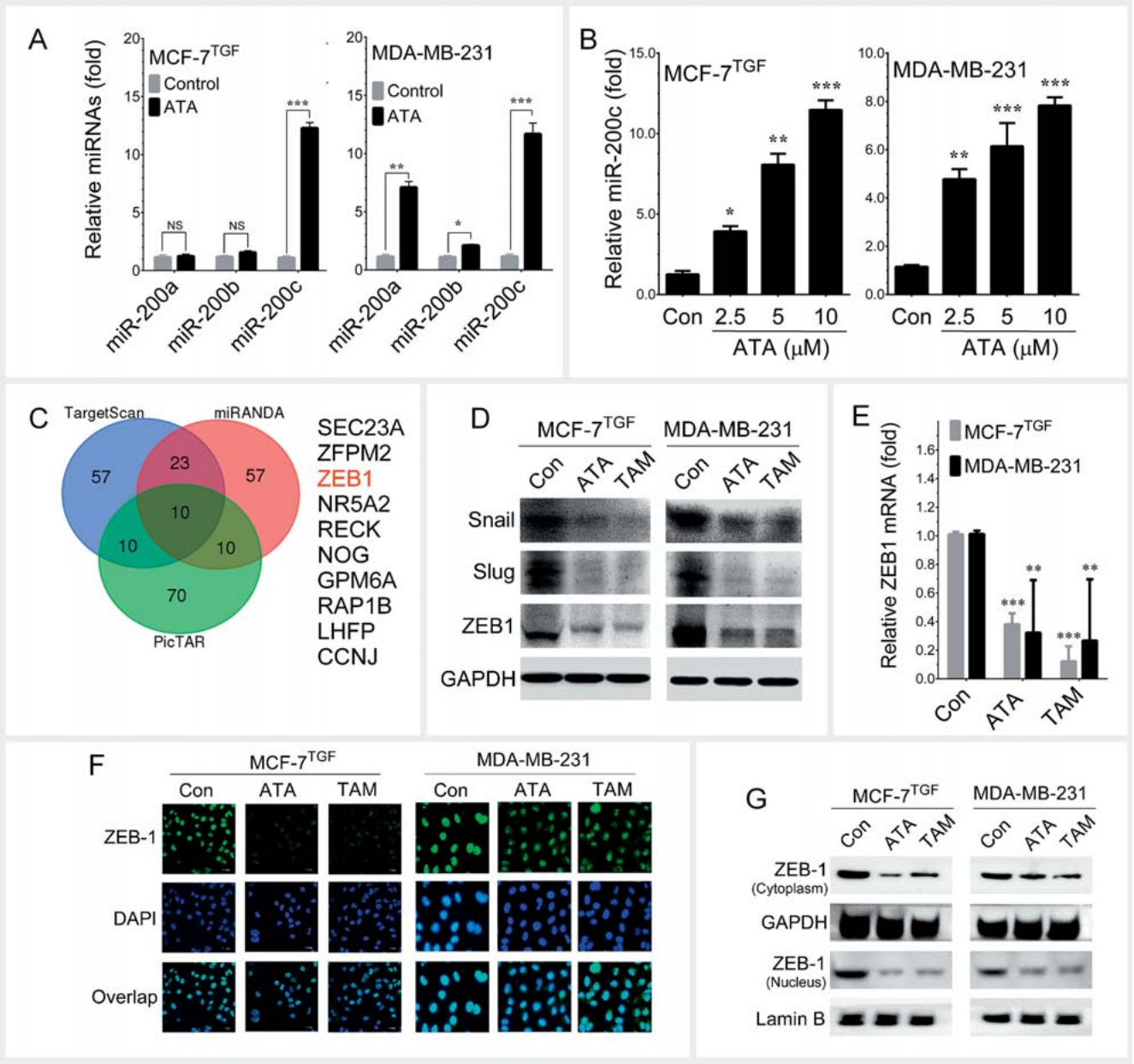

▶ **Fig. 3** ATA inhibits ZEB-1 via induction of miR-200c. **A** The effect of ATA on the miRNA-200 family genes including miR-200a, miR-200b, and miR-200c was examined in HBCCs. MCF-7^{TGF} and MDA-MB-231 cells were incubated with ATA (10 μM) or TAM (5 μM) for 24 h. Total RNA was prepared and q-PCR analysis was performed with corresponding primers. **B** The dose-dependent effect of ATA on miR-200c mRNA expression level in MCF-7^{TGF} and MDA-MB-231 cells was determined by q-PCR analysis. **C** Target prediction was performed using TargetScan, miRANDA, and PicTAR algorithms. **D** Protein expression levels of ZEB-1, snail, and slug were determined by western blot analysis. **E** The mRNA level of ZEB-1 was quantified by q-PCR analysis. **F** Cellular localization of ZEB-1 was determined by immunofluorescence analysis. **G** The nuclear translocation of ZEB-1 was examined by immunoblotting with cytoplasmic and nuclear fractions. Values represent the mean ± SD of 3 independent experiments. Statistical significance $^{***}p < 0.001$, $^{**}p < 0.01$, and $^{*}p < 0.05$ compared to control vs. sample treatment groups. NS: not statistically significant.

the translational level. ▶ **Fig. 2E** shows treatment with ATA significantly upregulated the protein levels of E-cadherin and occludin and downregulated ZO-1, N-cadherin, and vimentin levels in MCF-7^{TGF} and MDA-MB-231 cells. A similar regulatory effect of ATA was also observed in a dose-dependent manner (▶ **Fig. 2F**). Consistent with the morphological observation, the present data confirms that ATA regulates EMT/MET via dis-regulation of epithelial and mesenchymal markers in HBCCs.

As shown in ▶ **Fig. 3A**, treatment with ATA significantly upregulated miR-200c in MCF-7^{TGF} and MDA-MB-231 cells. This effect was also observed in a dose-dependent manner (▶ **Fig. 3B**). Next, in order to determine the downstream target genes of miR-200c, 3 target prediction algorithms (miRanda, TargetScan, and picTAR)

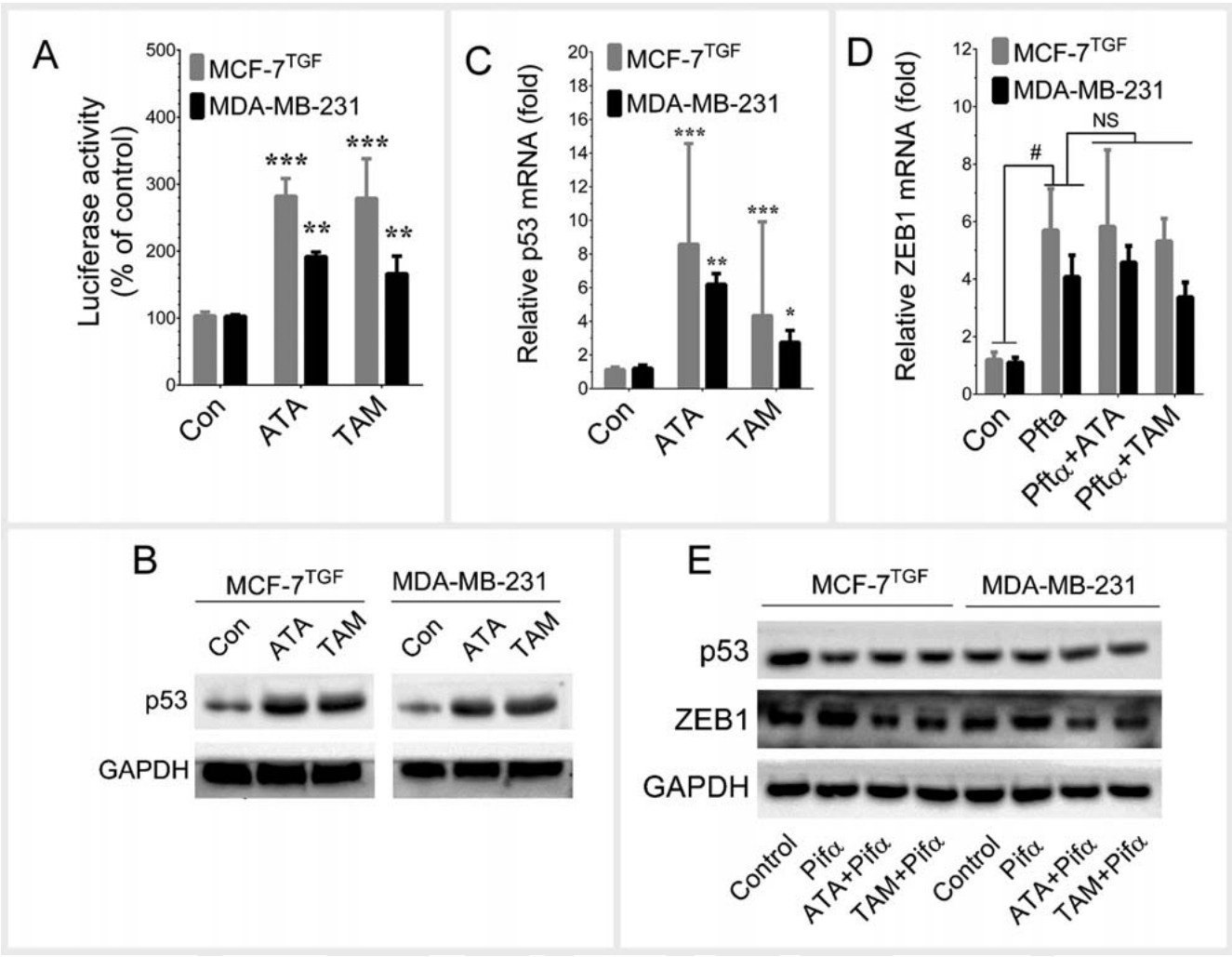

▶ **Fig. 4** ATA inhibits ZEB-1 through the activation of p53. MCF-7^{TGF} and MDA-MB-231 cells were incubated with ATA (10 µM) or TAM (5 µM) for 24 h. **A** Protein expression levels of p53 were determined by western blot analysis. **B** The transcriptional activity of p53 was measured by luciferase reporter assay. **C** The mRNA expression levels of p53 were quantified by q-PCR analysis. **D** To determine the involvement of p53 in ATA-mediated ZEB-1 inhibition, cells were pretreated with pifithrin-α (30 µM), a pharmacological inhibitor of p53, and then incubated with ATA (10 µM) or TAM (5 µM) for 24 h. The mRNA expression level of ZEB-1 was quantified by q-PCR. **E** The protein expression levels of ZEB-1 and p53 under pifithrin-α treatment were determined by western blot analysis. Values represent the mean ± SD of 3 independent experiments. Statistical significance $^{***}p < 0.001$, $^{**}p < 0.01$, and $^{*}p < 0.05$ compared to control vs. sample treatment groups. $^{\#}p < 0.001$ compared to control vs. pifithrin-α treatment group. NS: not statistically significant.

were applied. All 3 algorithms suggested that miR-200c could potentially target ZEB1 (▶ **Fig. 3C**), an important factor in breast cancer metastasis and a potential target for breast cancer therapy. As ZEB1 was a target gene of miR-200c, we then measured the effect of ATA on ZEB1 at transcriptional and translational levels. Treatment with ATA significantly decreased ZEB1 protein (▶ **Fig. 3D**) and mRNA (▶ **Fig. 3E**) expression levels in HBCCs. In addition, ATA significantly decreased other E-box-binding factors such as snail and slug in HBCCs (▶ **Fig. 3D**). Next, to determine the effects of ATA on ZEB1 transcriptional activity, the nuclear export was determined by immunofluorescence analysis. As shown in ▶ **Fig. 3F**, in control cells, a predominant level of ZEB1 was noted in the nucleus, whereas treatment with ATA significantly decreased ZEB1 level in the nucleus. Further confirmation with western blot analysis showed a similar result (i.e., treatment with ATA significantly inhibited ZEB1 levels in the cytoplasm and the nucleus (▶ **Fig. 3G**), which is directly associated with downregulation of ZEB1 mRNA by ATA).

The tumor suppressor gene product p53 has a role in EMT modulation through transcriptional activation of miR-200c [19]. Therefore, we hypothesize that ATA-mediated upregulation of miR-200c may be associated with activation of p53. As we expected, the luciferase reporter assay revealed that treatment with ATA significantly increased the transcriptional activity of p53 in both MCF-7^{TGF} and MDA-MB-231 cells (▶ **Fig. 4A**). This effect was further clarified by immunoblotting that ATA significantly increased p53 protein level in both cell lines (▶ **Fig. 4B**). This effect was further extended to the transcriptional level as ATA signifi-

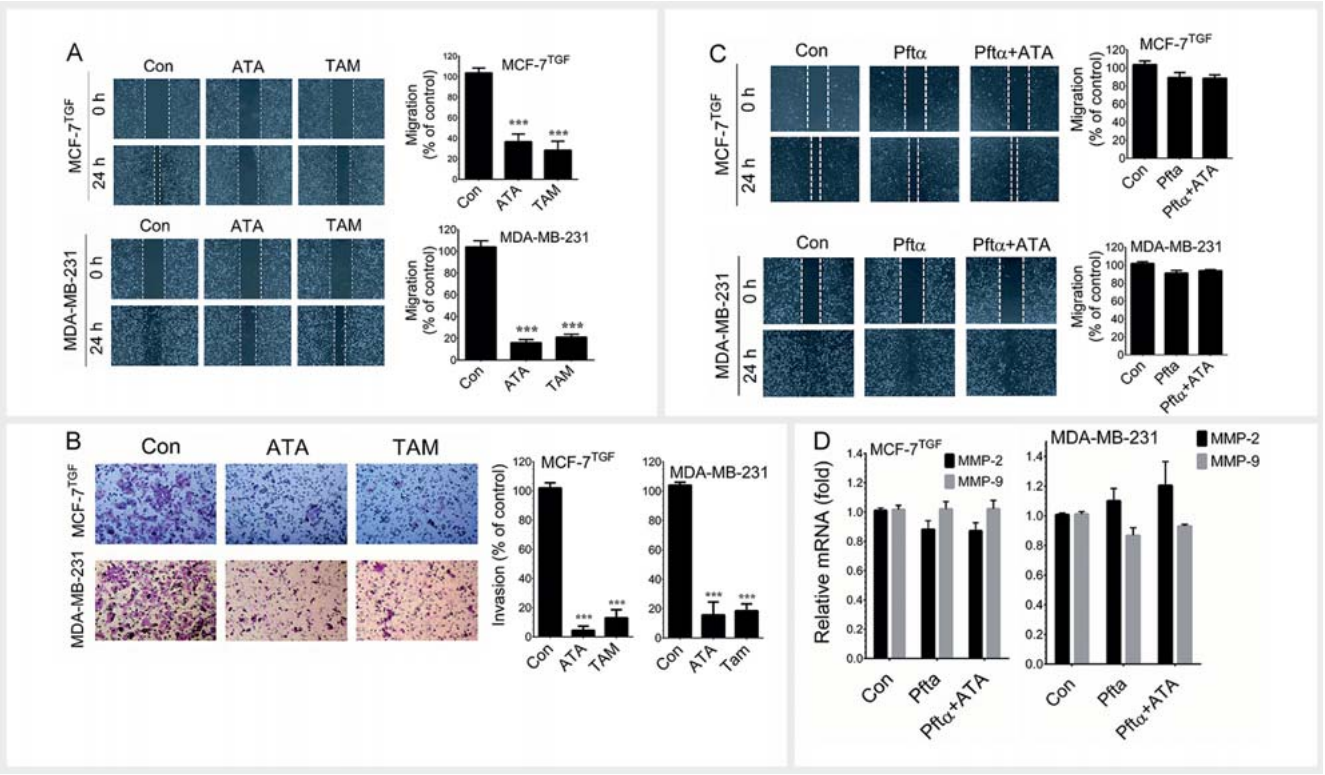

▶ **Fig. 5** ATA inhibits breast cancer cell migration and invasion *in vitro*. **A** The effect of ATA on HBCC migration was determined by wound healing assay. MCF-7^{TGF} and MDA-MB-231 cells were seeded into a 24-well culture plate with a silicon cell-free gap insert. After monolayer formation, the insert was removed and washed with PBS, and then the cells were treated with ATA (10 µM) or TAM (5 µM) for 24 h. The migrated cells were photographed (100× magnification) and the closure of the wounded area was calculated. The percentage of the wound closure area is presented as a histogram. **B** The effect of ATA on breast cancer invasion was determined by trans-well assay. ATA (10 µM) or TAM (5 µM) pre-treated cells were seeded into the upper chamber of a 24-well trans-well chamber containing DMEM with 1% FBS. The lower chamber was filled with complete serum media. The cells were allowed to invade for 24 h. Invading cells were then fixed and stained with Giemsa stain solution and counted in 5 random fields. The percentage of invasion is presented in histogram blot. **C** To determine the involvement of p53 in ATA-mediated inhibition of migration, cells were pretreated with pifithrin-α (30 µM) for 2 h and then incubated with ATA (10 µM) or TAM (5 µM) for 24 h. A wound healing assay was performed to determine the anti-migratory potential of ATA in p53 suppressed cells. **D** The mRNA expression levels of MMP-2 and MMP-9 in p53 suppressed cells were quantified by q-PCR. Values represent the mean ± SD of 3 independent experiments. Statistical significance $^{***}p < 0.001$ and $^{**}p < 0.01$ compared to control vs. sample treatment groups.

cantly increased p53 mRNA level in HBCCs (▶ **Fig. 4C**). To further define whether ATA-mediated inhibition of ZEB1 were through p53 activation, the expression level of ZEB1 was determined after treatment with ATA in the presence of pharmacological inhibitor of p53 (pifithrin-α, 30 µM). We found that ATA failed to inhibit ZEB1 mRNA (▶ **Fig. 4D**) and protein (▶ **Fig. 4E**) levels in the presence of p53 inhibitor. These inhibition experiments thus indicated that ATA-mediated upregulation of miR-200c and the following ZEB1 inhibition were through activation of p53.

In order to examine the effects of ATA on the motility of HBCCs, *in vitro* wound healing assay was performed. The effect of ATA on wound closure after 24 h was compared with control group, which was set up as 100%. As shown in ▶ **Fig. 5A**, MCF-7^{TGF} and MDA-MB-231 cells displayed aggressive motility as indicated by the area of wound closure, whereas treatment with ATA significantly reduced such capability. Histogram plot shows that treatment with ATA significantly reduced wound closure to 36.75 ± 3.6% and 16.03 ± 2.04% in MCF-7^{TGF} and MDA-MB-231 cells, respectively. Next, a trans-well invasion assay was performed to determine whether ATA could modulate the invasive capability of HBCCs. In agreement with the wound healing assay, treatment with ATA significantly suppressed the invasive potential of both MCF-7^{TGF} and MDA-MB-231 cells. Briefly, treatment with ATA significantly reduced the invasiveness of HBCCs to 4.41 ± 1.68% and 15.67 ± 5.11% in MCF-7^{TGF} and MDA-MB-231 cells, respectively (▶ **Fig. 5B**). We further examined whether ATA-induced p53 is involved in inhibition of breast cancer cell migration; cells were pretreated with pifithrin-α and then exposed to ATA for 24 h. As we expected, ATA failed to inhibit migration in pifithrin-α pre-treated cells (▶ **Fig. 5C**), which was further supported by unaltered expression levels of MMP-2 and MMP-9 in both cell lines (▶ **Fig. 5D**). These data suggest that ATA possess cell migration- and invasion-suppressing capabilities in HBCCs. This is consistent with the EMT regulatory effects of ATA.

Discussion

Accumulating scientific studies suggest that *A. cinnamomea* possesses various pharmacological properties, including anti-cancer effects, that go beyond its original usage. Among them, the anti-metastatic properties of *A. cinnamomea* are of particular interest. Recent studies have demonstrated that crude extracts or pure compounds have the ability of inhibit cancer cell metastasis via modulation of the EMT process [17, 20–22]. The anti-cancer properties of *A. cinnamomea* have been attributed to its unique composition of phytochemicals such as antroquinonols, antcins, and antrodins [12–15, 23, 24]. Among them, the antcins (ATA, antcin-B, antcin-C, antcin-D, antcin-E, antcin-F, antcin-G, antcin-H, antcin-I, antcin-K, and antcin M) are steroid-like compounds that exert various biological activities including, anti-inflammation [16, 25], hepatoprotection [26–28], anti-aging [29], anti-cancer [30–33], and anti-metastasis [34]. We have previously reported that ATA isolated from the fruiting bodies of *A. cinnamomea* inhibits inflammation in lung cells via mimicking a glucocorticoid receptor agonist, and this effect was highly comparable with synthetic steroids, such as cortisone and dexamethasone [16]. Recently we found that ATA inhibits proliferation and cancer stem cell-like phenotype of HBCCs via glucocorticoid-receptor-mediated induction of miR-708 *in vitro*. Treatment with ATA (10 mg/kg b. w.) twice a week for 10 wk significantly reduced tumor growth in HBCC xenograft mice. This study also concludes that administration of ATA up to a dose of 10 mg/kg was not a lethal dose for experimental mice, as indicated by no visible adverse effects or death, whereas less than 10 % of body weight loss was observed in the ATA treatment group [35]. In addition, a previous study has shown that antcin-K, isolated from the fruiting bodies of basswood-cultivated *A. cinnamomea*, inhibits human hepatoma cell metastasis via suppression of integrin-mediated adhesion, migration, and invasion [34]. Another study demonstrated that antcin-H from cultivated fruiting bodies of *A. cinnamomea* inhibits renal cancer cell invasion through inactivation of the FAK-ERK-C/EBP-β/c-Fos-MMP-7 pathways [31]. In the present study, we found that ATA inhibits metastasis of HBCCs.

Since the MCF-7 cell line represents epithelial morphology, upon stimulation with growth factors such as TGF-β1, the cells rapidly undergo phenotypic changes to a fibroblast or mesenchymal-like morphology, and such changes have been suggested to increase the aggressive ability of tumor cell metastasis [36]. Here, we found that TGF-β1-induced morphological changes in MCF-7 cells were significantly prevented by ATA, which is concomitant with our previous study that found in antrodin C, a maleimide derivative isolated from *A. cinnamomea*, inhibits TGF-β1-induced phenotypic changes in MCF-7 cells [17]. In addition, treatment with ATA induces MDA-MB-231 cells to change from a mesenchymal-like morphology to epithelial-like morphology. During the EMT processes, the epithelial marker proteins such as E-cadherin, occludin, cytokeratin, desmoplakin, entatin, and mucin-1 were downregulated, and the mesenchymal marker proteins including N-cadherin, vimentin, fibronectin, α-SMA, and β-catenin were upregulated [5]. Here, we found that ATA significantly upregulated E-cadherin and occludin and downregulated N-cadherin, ZO-1, and vimentin levels in MCF-7^{TGF} and MDA-MB-231 cells at both the protein and mRNA levels. These data provide strong evidence that ATA can modulate EMT processes in HBCCs.

Extensive studies have shown that phytochemicals may exert therapeutic effects by regulating miRNA expression [37]. Recent studies have shown that induction of miR-200c modulates EMT process in human breast and lung cancer cells [38, 39]. In the present study, we also found that miR-200c was significantly upregulated by ATA, which is correlated with reversed EMT processes. The miRNA-200 family has been shown to modulate EMT processes through directly targeting transcriptional repressors of E-cadherin, ZEB-1, and ZEB-2 in HBCCs [9]. We found that treatment with ATA significantly inhibited the transcriptional activity of ZEB-1 by blocking its nuclear export, as well as protein and mRNA expression in HBCCs. p53, a tumor suppressor gene product, has demonstrated its functional role in regulating EMT and EMT-associated stem cell-like properties via transcriptional activation of miR-200c [40]. Loss of p53 in breast cancer cells leads to decreased expression of miR-200c and activates the EMT processes and cancer stem cell-like phenotype [19, 41]. Here, we found that treatment with ATA significantly upregulates p53 activities in MCF-7^{TGF} and MDA-MB-231 cells, whereas pharmacological inhibition of p53 reduced ATA-medicated suppression of ZEB-1.

As tumor cell invasion and migration are also crucial steps involved in distant metastasis. Results of *in vitro* wound healing assay and trans-well invasion assay exhibited that ATA could reduce the migration and invasion abilities of HBCCs. Further studies revealed that ATA-mediated inhibition of migration and invasion is associated with downregulation of MMPs, including MMP-2 and MMP-9. In addition, ATA failed to inhibit migration and invasion of HBCCs under p53 knock-down. Our results were consistent with previous reports that induction of p53 downregulates MMPs activity and inhibits tumor cell invasion [42].

The EMT modulation, anti-migration, and anti-invasive potentials of ATA were highly comparable with known anti-metastatic drug TAM. TAM has been reported to modulate EMT processes in triple-negative breast cancer cells by methylating miR-200c [38]. Despite the beneficial effects, TAM use is often linked to adverse side effects, including increased tumor or bone pain, uterine endometrial cancer, and nonalcoholic fatty liver diseases [43]. We previously reported that ATA possessed anti-inflammation and anti-tumor effects [16, 35] and other related antcins, such as antcin-B, -C, -H, and -K exhibited hepatoprotective effects [26, 27, 44, 45]. Presumably, ATA could not produce such side effects. However, further toxicological assessments are highly warranted to support this notion.

Taken together, our data suggest that ATA may produce its anti-migration and anti-invasive effects by regulating the EMT process through the modulation of EMT regulatory proteins, including E-cadherin, occludin, N-cadherin, and vimentin via transcriptional inactivation of ZEB-1. This effect was strongly associated with p53-mediated miR-200c activation. In addition, ATA blocked tumor cell invasion and migration potential of HBCCs via p53-mediated inhibition of MMPs. These lines of evidence suggest that ATA could be a promising candidate for the development of chemotherapeutic/chemo-preventive agents for the treatment of

▶ **Table 1** List of primers used in this study.

qRT-PCR primer sequences		
	Forward	**Reverse**
miR-200a	5′-GCCGTCTAACACTGTCTGGTA-3′	5′-CCTACGCCACAATTAACAAGCC-3′
miR-200b	5′-GCG GCT AAT ACT GCC TGG TAA-3′	5′-GTG CAG GGT CCG AGG T-3′
miR-200c	5′-CCAACGTAATACTGCCGGGT-3′	5′-CTGCTGGCGAATTAGTAGACCA-3′
E-cadherin	5′-TGCTCACATTTCCCAACTC-3′	5′-TCTGTCACCTTCAGCCATC-3′
Vimentin	5′-CCAGGCAAAGCAGGAGGTC-3′	5′-GGGTATCAACCAGAGGGAGT-3′
MMP-2	5′-CTCATCGCAGATGCCTGGAA-3′	5′-TTCAGGTAATAGGCACCCTTGAAGA-3′
MMP-9	5′-ACGCACGACGTCTTCCAGTA-3′	5′-CCACCTGGTTCAACTCACTCC-3′
ZEB-1	5′-GCACAACCAAGTGCAGAAGA-3′	5′-CATTTGCAGATTGAGGCTGA-3′
p53	5′-CCGCAGTCAGATCCTAGCG-3′	5′-AATCATCCATTGCTTGGGACG-3′
GAPDH	5′-TCCTGGTATGACAACGAAT-3′	5′-GGTCTCTCTCTTCCTCTTG-3′

human breast cancers. However, further experimental studies are needed to explore its efficacy in *in vivo* models.

Materials and Methods

Chemicals and reagents

ATA was isolated from the fruiting bodies of *A. cinnamomea*, as described previously [16]. Briefly, the oven-dried fruiting bodies of *A. cinnamomea* (50 g) were extracted with MeOH at room temperature for 7 consecutive days. The companied extracts were evaporated under reduced pressure. The brown sediment was re-suspended in H_2O and then extracted with EtOAc and *n*-BuOH sequentially. The EtOAc fraction was subjected to silica gel chromatography using gradient mixture of *n*-hexane and EtOAc as eluent. It produced 10 fractions. Fraction 5 (n-hexane and EtOAc with a ratio of 8:2) was further purified by silica gen column and eluted with CH_2Cl_2-EtOAc, which produced 6 subfractions (5A-5F). Subfraction 5C was subjected to semi-preparative HPLC and eluted with CH_2Cl_2-acetone (40:1) to yield ATA (5.1 g). The purity of ATA was above 99% according to HPLC and ^{1}H-NMR analyses. MEM and RPMI medium, FBS, sodium pyruvate, penicillin, and streptomycin were obtained from Invitrogen. TAM (purity > 99%), MTT, DAPI, and pifithrin-α were purchased from Sigma-Aldrich. TGF-β1 was bought from R&D Systems. Antibodies against E-cadherin, GAPGH, N-cadherin, occludin, p53, slug, snail, vimentin, ZEB-1, and ZO-1 were obtained from Cell Signaling Technology Inc. All other chemicals were reagent-grade or HPLC grade and supplied by either Merck or Sigma-Aldrich.

Cell culture and sample treatment

The HBCC lines MCF-7 and MDA-MB-231 were obtained from the Bioresource Collection and Research Center. MCF-7 and MDA-MB-231 cells were grown in MEM and RPMI medium, respectively. Both mediums were supplemented with 10% FBS, 1.5 g/L sodium bicarbonate, and 100 U/L penicillin and streptomycin at 37 °C in a humidified atmosphere of 5% CO_2. Cells were treated with ATA (10 µM) or TAM (5 µM) for 24 h, and 0.1% DMSO was used as a vehicle control. MCF-7 cells were stimulated with 10 ng/mL of TGF-β1 and the TGF-β1 stimulated MCF-7 cells were represented as MCF-7^{TGF}.

Cell viability assay

Cell viability was determined by MTT colorimetric assay as described previously [17]. Briefly, MCF-7 and MDA-MB-231 cells were seeded in a 96-well plates at a density of 1×10^4 cells/well for 24 h. Cells were then treated with various concentrations of ATA (1, 5, and 10 µM) for 24 h. After incubation, the medium-deprived cells were incubated with 0.5 mg/mL 0 f MTT in 200 µL of fresh medium for 2 h at 37 °C. The MTT-generated formazan crystals were dissolved in DMSO and the absorbance was measured at 570 nm (A_{570}) using an ELISA microplate reader (µQuant, Bio-Tek Instruments). The percentage of cell viability was calculated as: (A_{570} of treated cells/A_{570} of untreated cells) × 100.

Phase contrast microscopy

The phenotypic changes of HBCCs were determined by phase contrast microscopy MCF-7^{TGF} and MDA-MB-231 cells were incubated with either ATA (10 µM) or TAM (5 µM) for 24 h. The morphological changes were visualized by phase contrast microscopy. The images were collected using Motic inverted microscope.

F-actin staining and immunofluorescence

F-action staining by Phalloidin was described previously [17]. Briefly, MCF-7^{TGF} and MDA-MB-231 cells were seeded at a density of 2×10^4 cells/well in 8-well glass Nunc Lab-Tek chamber slide (Thermo Fisher Scientific) for 24 h. Then the cells were exposed to either ATA (10 µM) or TAM (5 µM) for 24 h. Sample treated cells were rinsed with PBS, fixed in 4% paraformaldehyde for 15 min at room temperature, permeabilized with Triton X-100 in PBS for 10 min, and incubated with 6% BSA for 1 h. Then the cells were washed with PBS and incubated with 660 nM of Alexa Flour 488 Phalloidin (Thermo Fisher Scientific) in 100 µL of 6% BSA for 15 min to stain for F-actin and visualized using a fluorescence microscope (Motic Electric Group) at 40× magnification. For the immunofluorescence analysis, cells were incubated with the corresponding primary antibodies with a dilution ratio of 1:200 in 1.5% FBS. The cells were then incubated with FITC-conjugated

secondary antibody (Alexa Flour 488, 1 : 1000) for another 1 h in 6% BSA. Then the cells were stained with 1 µg/mL DAPI for 5 min and washed with PBS. The fluorescent cell images were visualized by a confocal fluorescence microscope (Leica TCS-SP5-X AOBS) and images were processed by Image Pro Plus version 6.1 software (Media Cybernetics). Emission detection range was set as 457–522 nm for FITC and 405–464 for DAPI with 200 MHz of gain.

Immunoblotting

Total cell lysates were prepared using RIPA lysis buffer (Thermo Fisher Scientific). The cytoplasmic and nuclear fractions were obtained by NE-PER Nuclear and Cytoplasmic Protein Extraction Reagent kit (Pierce Biotechnology). Protein concentration was determined by Bio-Rad protein assay reagent (Bio-Rad Laboratories). Equal amounts of denatured protein samples (60 µg) were separated by 7–12% SDS-PAGE and the separated proteins were transferred onto PVDF membrane overnight. Then the membranes were blocked with 5% nonfat dried milk for 30 min, followed by incubation with specific primary antibodies (1 : 1000) in PBS for overnight, and incubated with either horseradish peroxidase conjugated goat anti-rabbit or anti-mouse antibodies (1 : 10 000) in PBS for 1 h. The immunoblots were developed with the enhanced chemiluminescence reagent (Millipore) and images were captured by VL Chemi-Smart 3000 docking system (Viogene Biotek).

Quantitative real-time PCR

Total RNA was extracted by Trizol Reagent (Thermo Fisher Scientific). RNA concentration was quantified with a NanoVue Plus spectrophotometer (GE Health Care Life Sciences, Chicago, IL). q-PCR was performed on a real-time PCR detection system and software (Applied Biosystems). First-strand cDNA was generated by SuperScript III reverse transcriptase kit (Invitrogen). Quantification of mRNA expression for genes of interest was performed by q-PCR reactions with equal volume of cDNA, forward and reverse primers (10 µM), and power SYBR Green Master Mix (Applied Biosystems). The mRNA levels were normalized with GAPDH, while miRNA levels were normalized with U6. The primer sequences of each gene for q-PCR are summarized in ▶ **Table 1**.

Luciferase reporter assay

The transcriptional activity of p53 was determined by commercially available luciferase reporter assay kits (Cignal p53 pathway reporter assay kit, Quiagen). Briefly, sample-treated MCF-7^{TGF} and MDA-MB-231 cells were transfected with Cignal p53 reporter and luciferase activity was measured using Dual Luciferase Assay system (Promega) and the relative luminescence intensity was measured using a fluorescence spectrophotometer (Hidex Oy). Firefly luciferase experimental reporter was normalized to Renilla luciferase activity to control transfection efficiency.

In vitro wound healing assay

MCF-7^{TGF} and MDA-MB-231 cells (1×10^4 cells/well) were seeded into a 24-well culture plate with silicon cell-free gap insert (ibidi GmbH). After cells adhered to the culture plate, the silicon insert was removed, washed with PBS, and then cells were treated with ATA or TAM or transiently transfected with anti-miRNAs for 24 h. The migrated cells were photographed (100× magnification) at 0 and 24 h to monitor the migration of cells into the wounded area, and the closure of the wounded area was calculated.

Trans-well migration assay

The invasive ability of breast cancer cells was quantified using Matrigel invasion assay. Briefly, 10 µL (0.5 mg/mL) BD Matrigel Basement Membrane Matrix (BD Bioscience) was applied to 8-µm polycarbonate membrane filters and the inserts were placed on 12-well culture plates. On the other hand, MCF-7^{TGF} and MDA-MB-231 cells were treated with either ATA or TAM or transiently transfected with anti-miRNAs for 24 h. After treatment, cells were collected by trypsin. A total of 2×10^5 cells in fresh medium without serum (200 µL) were added to the Matrigel coated filters (upper chamber), and 750 µL of completed medium was added to the lower chamber as a chemoattractant. The plates were incubated at 37 °C for 24 h. After incubation, the cells remaining on the upper surface of the membrane were removed with cotton swabs, and the cells that had migrated to the lower side of the membrane were fixed using methanol and stained with Giemsa solution for 15 min at room temperature. The invaded cells on the bottom of the membrane were washed with PBS and photographed under a confocal microscope (magnification, 100×).

Computational target prediction algorithm for miR-200c targets

Predicting target genes of miRNAs by computational algorithm is considered as a comprehensive probabilistic parameter for understanding their biological functions. To identify target genes that miR-200c regulate are generated by 3 target prediction algorithms (PicTar, Targetscan, and miRANADA) [46]. The first 100 picks from the combined 3 algorithms were selected. Next, number of genes found in overlapped 3 algorithms (10 genes) were cross checked existing experimental results, particularly genes involved in metastasis of cancer cells.

Statistical analysis

Data are expressed as mean ± standard deviation (SD). All data were analyzed using the statistical software GraphPad Prism version 6.0 for Windows (GraphPad Software). Statistical analysis was performed using one-way analysis of variance followed by Dunnett's test for multiple comparison. A p-values of less than 0.05*, 0.01**, and 0.001*** was considered statistically significant for the ATA or TAM or anti-miR treatment group versus the control group.

Acknowledgements

This study was supported by the Ministry of Science and Technology, Taiwan, (106-2313-B-005-012-MY3).

Conflict of Interest

The authors declare that there are no conflicts of interest.

References

[1] International Agency for Research on Cancer. Cancer Tomorrow 2018: estimated number of incident cases from 2018 to 2030, breast, females, all ages. Available at http://gco.iarc.fr/tomorrow. Accessed September 12, 2018

[2] Siegel RL, Miller KD, Jemal A. Cancer statistics, 2019. CA Cancer J Clin 2019; 69: 7–34

[3] DeSantis CE, Bray F, Ferlay J, Lortet-Tieulent J, Anderson BO, Jemal A. International variation in female breast cancer incidence and mortality rates. Cancer Epidemiol Biomarkers Prev 2015; 24: 1495–1506

[4] Weigelt B, Peterse JL, van 't Veer LJ. Breast cancer metastasis: markers and models. Nat Rev Cancer 2005; 5: 591–602

[5] Lamouille S, Xu J, Derynck R. Molecular mechanisms of epithelial-mesenchymal transition. Nat Rev Mol Cell Biol 2014; 15: 178–196

[6] Croce CM. Causes and consequences of microRNA dysregulation in cancer. Nat Rev Genet 2009; 10: 704–714

[7] Ma L. MicroRNA and metastasis. Adv Cancer Res 2016; 132: 165–207

[8] Park SM, Gaur AB, Lengyel E, Peter ME. The miR-200 family determines the epithelial phenotype of cancer cells by targeting the E-cadherin repressors ZEB1 and ZEB2. Genes Dev 2008; 22: 894–907

[9] Weidle UH, Dickopf S, Hintermair C, Kollmorgen G, Birzele F, Brinkmann U. The role of micro RNAs in breast cancer metastasis: preclinical validation and potential therapeutic targets. Cancer Genom Proteom 2018; 15: 17–39

[10] Abbasi B, Iqbal J, Mahmood T, Khalil A, Ali B, Kanwal S, Shah S, Ahmad R. Role of dietary phytochemicals in modulation of miRNA expression: natural swords combating breast cancer. Asian Pac J Trop Med 2018; 11: 501–509

[11] Ao ZH, Xu ZH, Lu ZM, Xu HY, Zhang XM, Dou WF. Niuchangchih (*Antrodia camphorata*) and its potential in treating liver diseases. J Ethnopharmacol 2009; 121: 194–212

[12] Geethangili M, Tzeng YM. Review of pharmacological effects of *Antrodia camphorata* and its bioactive compounds. Evid Based Complement Alternat Med 2011; 2011: 17

[13] Lu MC, El-Shazly M, Wu TY, Du YC, Chang TT, Chen CF, Hsu YM, Lai KH, Chiu CP, Chang FR, Wu YC. Recent research and development of *Antrodia cinnamomea*. Pharmacol Ther 2013; 139: 124–156

[14] Shanmugavadivu M, Velmurugan BK. Pharmalogical activities of antroquinonol – mini review. Chem Biol Interact 2018; 297: 8–15

[15] Zhang BB, Hu PF, Huang J, Hu YD, Chen L, Xu GR. Current advances on the structure, bioactivity, synthesis, and metabolic regulation of novel ubiquinone derivatives in the edible and medicinal mushroom *Antrodia cinnamomea*. J Agric Food Chem 2017; 65: 10395–10405

[16] Chen YC, Liu YL, Li FY, Chang CI, Wang SY, Lee KY, Li SL, Chen YP, Jinn TR, Tzen JT. Antcin A, a steroid-like compound from *Antrodia camphorata*, exerts anti-inflammatory effect via mimicking glucocorticoids. Acta Pharmacol Sin 2011; 32: 904–911

[17] Kumar KJ, Vani MG, Chueh PJ, Mau JL, Wang SY. Antrodin C inhibits epithelial-to-mesenchymal transition and metastasis of breast cancer cells via suppression of Smad2/3 and beta-catenin signaling pathways. PLoS One 2015; 10: e0117111

[18] Manni A. Tamoxifen therapy of metastatic breast cancer. J Lab Clin Med 1987; 109: 290–299

[19] Chang CJ, Chao CH, Xia W, Yang JY, Xiong Y, Li CW, Yu WH, Rehman SK, Hsu JL, Lee HH, Liu M, Chen CT, Yu D, Hung MC. p53 regulates epithelial-mesenchymal transition and stem cell properties through modulating miRNAs. Nat Cell Biol 2011; 13: 317–323

[20] Hseu YC, Chang GR, Pan JY, Rajendran P, Mathew DC, Li ML, Liao JW, Chen WT, Yang HL. *Antrodia camphorata* inhibits epithelial-to-mesenchymal transition by targeting multiple pathways in triple-negative breast cancers. J Cell Physiol 2019; 234: 4125–4139

[21] Hseu YC, Chao YH, Lin KY, Way TD, Lin HY, Thiyagarajan V, Yang HL. *Antrodia camphorata* inhibits metastasis and epithelial-to-mesenchymal transition via the modulation of claudin-1 and Wnt/beta-catenin signaling pathways in human colon cancer cells. J Ethnopharmacol 2017; 208: 72–83

[22] Liu YM, Liu YK, Huang PI, Tsai TH, Chen YJ. *Antrodia cinnamomea* mycelial fermentation broth inhibits the epithelial-mesenchymal transition of human esophageal adenocarcinoma cancer cells. Food Chem Toxicol 2018; 119: 380–386

[23] Liu YW, Lu KH, Ho CT, Sheen LY. Protective effects of *Antrodia cinnamomea* against liver injury. J Tradit Complement Med 2012; 2: 284–294

[24] Yue PY, Wong YY, Chan TY, Law CK, Tsoi YK, Leung KS. Review of biological and pharmacological activities of the endemic Taiwanese bitter medicinal mushroom, *Antrodia camphorata* (M. Zang et C. H. Su) Sh. H. Wu et al. (higher Basidiomycetes). Int J Med Mushrooms 2012; 14: 241–256

[25] Lu ZM, Xu ZH. Antcin A contributs to anti-inflammatory effect of Niuchangchih (*Antrodia camphorata*). Acta Pharmacol Sin 2011; 32: 981–982

[26] Gokila Vani M, Kumar KJ, Liao JW, Chien SC, Mau JL, Chiang SS, Lin CC, Kuo YH, Wang SY. Antcin C from *Antrodia cinnamomea* protects liver cells against free radical-induced oxidative stress and apoptosis *in vitro* and *in vivo* through Nrf2-dependent mechanism. Evid Based Complement Alternat Med 2013; 2013: 296082

[27] Huo Y, Win S, Than TA, Yin S, Ye M, Hu H, Kaplowitz N. Antcin H protects against acute liver injury through disruption of the interaction of c-Jun-N-terminal kinase with mitochondria. Antioxid Redox Signal 2017; 26: 207–220

[28] Tien AJ, Chien CY, Chen YH, Lin LC, Chien CT. Fruiting bodies of *Antrodia cinnamomea* and its active triterpenoid, antcin K, ameliorates N-nitrosodiethylamine-induced hepatic inflammation, fibrosis and carcinogenesis in Rats. Am J Chin Med 2017; 45: 173–198

[29] Senthil KK, Gokila VM, Mau JL, Lin CC, Chu FH, Wei CC, Liao VH, Wang SY. A steroid like phytochemical antcin M is an anti-aging reagent that eliminates hyperglycemia-accelerated premature senescence in dermal fibroblasts by direct activation of Nrf2 and SIRT-1. Oncotarget 2016; 7: 62836–62861

[30] Chen YF, Chang CH, Huang ZN, Su YC, Chang SJ, Jan JS. The JAK inhibitor antcin H exhibits direct anticancer activity while enhancing chemotherapy against LMP1-expressed lymphoma. Leuk Lymphoma 2019; 60: 1193–1203

[31] Chiu KY, Chen TH, Wen CL, Lai JM, Cheng CC, Liu HC, Hsu SL, Tzeng YM. Antcin-H isolated from *Antrodia cinnamomea* inhibits renal cancer cell invasion partly through inactivation of FAK-ERK-C/EBP-beta/c-Fos-MMP-7 pathways. Evid Based Complement Alternat Med 2017; 2017: 5052870

[32] Hsieh YC, Rao YK, Whang-Peng J, Huang CY, Shyue SK, Hsu SL, Tzeng YM. Antcin B and its ester derivative from *Antrodia camphorata* induce apoptosis in hepatocellular carcinoma cells involves enhancing oxidative stress coincident with activation of intrinsic and extrinsic apoptotic pathway. J Agric Food Chem 2011; 59: 10943–10954

[33] Lai CI, Chu YL, Ho CT, Su YC, Kuo YH, Sheen LY. Antcin K, an active triterpenoid from the fruiting bodies of basswood cultivated *Antrodia cinnamomea*, induces mitochondria and endoplasmic reticulum stress-mediated apoptosis in human hepatoma cells. J Tradit Complement Med 2016; 6: 48–56

[34] Huang YL, Chu YL, Ho CT, Chung JG, Lai CI, Su YC, Kuo YH, Sheen LY. Antcin K, an Active triterpenoid from the fruiting bodies of basswood-cultivated *Antrodia cinnamomea*, inhibits metastasis via suppression of integrin-mediated adhesion, migration, and invasion in human hepatoma cells. J Agric Food Chem 2015; 63: 4561–4569

[35] Senthil Kumar KJ, Gokila Vani M, Hsieh HW, Lin CC, Liao JW, Chueh PJ, Wang SY. MicroRNA-708 activation by glucocorticoid receptor agonists regulate breast cancer tumorigenesis and metastasis via downregulation of NF-kappaB signaling. Carcinogenesis 2019; 40: 335–348

[36] Lv ZD, Kong B, Li JG, Qu HL, Wang XG, Cao WH, Liu XY, Wang Y, Yang ZC, Xu HM, Wang HB. Transforming growth factor-beta 1 enhances the invasiveness of breast cancer cells by inducing a Smad2-dependent epithelial-to-mesenchymal transition. Oncol Rep 2013; 29: 219–225

[37] Srivastava SK, Arora S, Averett C, Singh S, Singh AP. Modulation of microRNAs by phytochemicals in cancer: underlying mechanisms and translational significance. BioMed Res Inter 2015; 2015: 9

[38] Wang Q, Cheng Y, Wang Y, Fan Y, Li C, Zhang Y, Wang Y, Dong Q, Ma Y, Teng YE, Qu X, Liu Y. Tamoxifen reverses epithelial-mesenchymal transition by demethylating miR-200c in triple-negative breast cancer cells. BMC Cancer 2017; 17: 492

[39] Liu PL, Liu WL, Chang JM, Chen YH, Liu YP, Kuo HF, Hsieh CC, Ding YS, Chen WW, Chong IW. MicroRNA-200c inhibits epithelial-mesenchymal transition, invasion, and migration of lung cancer by targeting HMGB1. PLoS One 2017; 12: e0180844

[40] Schubert J, Brabletz T. p53 Spreads out further: suppression of EMT and stemness by activating miR-200c expression. Cell Res 2011; 21: 705–707

[41] Knezevic J, Pfefferle AD, Petrovic I, Greene SB, Perou CM, Rosen JM. Expression of miR-200c in claudin-low breast cancer alters stem cell functionality, enhances chemosensitivity and reduces metastatic potential. Oncogene 2015; 34: 5997–6006

[42] Zhu H, Evans B, O'Neill P, Ren X, Xu Z, Hait WN, Yang JM. A role for p53 in the regulation of extracellular matrix metalloproteinase inducer in human cancer cells. Cancer Biol Ther 2009; 8: 1722–1728

[43] Gu W, Xu W, Sun X, Zeng B, Wang S, Dong N, Zhang X, Chen C, Yang L, Chen G, Xin A, Ni Z, Wang J, Yang J. Anordrin eliminates tamoxifen side effects without changing its antitumor activity. Sci Rep 2017; 7: 43940

[44] Wu Y, Tian WJ, Gao S, Liao ZJ, Wang GH, Lo JM, Lin PH, Zeng DQ, Qiu DR, Liu XZ, Zhou M, Lin T, Chen HF. Secondary metabolites of petri-dish cultured *Antrodia camphorata* and their hepatoprotective activities against alcohol-induced liver injury in mice. Chin J Nat Med 2019; 17: 33–42

[45] Li ZW, Kuang Y, Tang SN, Li K, Huang Y, Qiao X, Yu SW, Tzeng YM, Lo JY, Ye M. Hepatoprotective activities of *Antrodia camphorata* and its triterpenoid compounds against CCl4-induced liver injury in mice. J Ethnopharmacol 2017; 206: 31–39

[46] Zhang Y, Verbeek FJ. Comparison and integration of target prediction algorithms for microRNA studies. J Integr Bioinform 2010; 7: 127